

**Confining Dirac electrons on a topological insulator surface using potentials and a magnetic field**

Ranjani Seshadri and Diptiman Sen

*Centre for High Energy Physics, Indian Institute of Science, Bangalore 560 012, India*

(Received 19 April 2014; revised manuscript received 14 May 2014; published 12 June 2014)

We study the effects of extended and localized potentials and a magnetic field on the Dirac electrons residing at the surface of a three-dimensional topological insulator like  $\text{Bi}_2\text{Se}_3$ . We use a lattice model to numerically study the various states; we show how the potentials can be chosen in a way which effectively avoids the problem of fermion doubling on a lattice. We show that extended potentials of different shapes can give rise to states which propagate freely along the potential but decay exponentially away from it. For an infinitely long potential barrier, the dispersion and spin structure of these states are unusual and these can be varied continuously by changing the barrier strength. In the presence of a magnetic field applied perpendicular to the surface, these states become separated from the gapless surface states by a gap, thereby giving rise to a quasi-one-dimensional system. Similarly, a magnetic field along with a localized potential can give rise to exponentially localized states which are separated from the surface states by a gap and thereby form a zero-dimensional system. Finally, we show that a long barrier and an impurity potential can produce bound states which are localized at the impurity, and an “L”-shaped potential can have both bound states at the corner of the L and extended states which travel along the arms of the potential. Our work opens the way to constructing wave guides for Dirac electrons.

DOI: [10.1103/PhysRevB.89.235415](https://doi.org/10.1103/PhysRevB.89.235415)

PACS number(s): 73.20.-r, 73.40.-c

**I. INTRODUCTION**

Topological insulators (TIs) are materials which have gapped states in the bulk and gapless states on the boundaries which are protected by time-reversal symmetry [1,2]. These materials have been studied both theoretically [3–7] and experimentally [8–11] for a number of years. Three-dimensional TIs such as  $\text{Bi}_2\text{Se}_3$ ,  $\text{Bi}_2\text{Te}_3$ , and  $\text{Sb}_2\text{Te}_3$  have surfaces on which there is a single species of gapless states which is governed by the Dirac equation [9–11]. A number of interesting properties of the surface states of a TI have been studied [1,2,11–23]. Junctions of different surfaces of TIs, sometimes separated by a geometrical step or a magnetic domain wall [24–32], junctions of surfaces of a TI with normal metals or magnetic materials [33] or superconductors [34], and polyhedral surfaces [35] have been investigated. The effects of finite sizes [36–41] and different orientations [30,42–45], and transport around different surfaces of a TI in the presence of a magnetic field [46] have been studied. The effect of a periodically varying one-dimensional potential and a magnetic field on the spectrum of electrons on the surface of  $\text{Bi}_2\text{Te}_3$  has been studied in Ref. [47].

It is known analytically that an infinitely long  $\delta$ -function potential barrier running along the  $x$  axis applied to the  $x$ - $y$  surface of a TI gives rise to states which propagate as plane waves along the barrier and decay exponentially away from it [25]. However, there is no energy gap between these localized states produced by the potential barrier and the gapless surface states which exist far from the potential. As a result, even a weak disorder can scatter the localized states into the surface states; the localized states are therefore not robust against disorder. On the other hand, a potential localized in a two-dimensional region does not produce any localized states at all for Dirac electrons. If we now apply a Zeeman field perpendicular to the surface, the surface states get gapped out. It is then possible that localized potentials will also produce localized states, and that the states produced by various potentials (either extended or localized) will lie in

the gap of the surface states; energy conservation will then not allow impurity-induced scattering between the localized and surface states. The localized states will therefore be stable against weak disorder for energetic reasons.

The purpose of this paper is to show how Dirac electrons can be confined within various geometrical regions using potentials barriers of different shapes and a perpendicular magnetic field. In particular, we will show that Dirac electrons can be confined to one or zero dimensions, resembling systems of quantum wires and dots. The one-dimensional system can even have bends through which the electrons can propagate. (This may be useful for various practical applications; by combining a series of localized potentials, we can construct a wave guide or a network of wave guides for Dirac electrons.) We will use a lattice model to carry out our calculations since such a model allows us to numerically study the effects of potentials of any magnitude and shape.

We should point out here that although the energy gap produced by a magnetic field protects the localized states from scattering to the surface states, there is no protection against scattering between two localized states lying at the same energy, say, at momenta  $+k$  and  $-k$ . As we will see below, this is because the spins of the states at  $\pm k$  do not point opposite to each other when a magnetic field is present, and a nonmagnetic impurity can therefore cause a transition between the two states. In this sense, our localized states do not enjoy topological protection, in contrast to states bound to a dislocation line in a three-dimensional TI which are topologically protected [48].

The plan of our paper is as follows. In Sec. II, we review the Dirac Hamiltonian in the continuum and its symmetries in the presence of a potential and a magnetic field. In Sec. III we discretize the Hamiltonian using a square lattice and we discuss the fermion doubling problem that arises for Dirac electrons. In Sec. IV, we numerically study the spectrum of electrons in the presence of an infinitely long potential barrier which is taken to have a Gaussian profile in the transverse direction. Since this system has translation invariance along one direction, the

momentum along that direction is a good quantum number and can be used to reduce it to a one-dimensional problem. In the absence of a magnetic field, the dispersion of the states propagating along the barrier (henceforth called edge states) is qualitatively found to be of the form  $E = v|k_x|$ , where  $k_x$  is the momentum along the barrier, if  $|k_x|$  is much smaller than the inverse lattice spacing. The expectation value of the spin,  $\langle \vec{\sigma} \rangle$ , of the edge states lies in the  $y$  direction. The velocity  $v$  of the edge states is smaller than that of the surface states and it can be varied by changing the strength of the potential barrier. The velocity  $v$  is found to be very small for a particular value of the potential barrier, giving rise to an almost flat band near  $E = 0$ . The wave function of the edge states decays exponentially away from the potential barrier; the decay length is found to be inversely proportional to  $|k_x|$ . Hence the edge states will cease to exist when the decay length becomes comparable to the size of the system. When a Zeeman field is applied in the  $z$  direction, the surface states become gapped but the edge states do not. Further, the edge state now exists even for  $k_x = 0$ , and their dispersion can be controlled by the potential barrier. The edge states then define a tunable one-dimensional system which is separated from the surface states by a gap. In Sec. V, we study the effects of a variety of potentials with two-dimensional profiles. We first consider a potential localized in some region. In the absence of a Zeeman field there are no localized states, but when a Zeeman field is turned on, we find that there exponentially localized states can appear if the potential is strong enough. Next, we study a combination of a long potential barrier, a localized potential, and a magnetic field; we find that states can appear which are bound to the localized potential. Finally, we study what happens if there is an “L”-shaped potential consisting of two infinitely long arms meeting at a corner and a magnetic field. We find that there can be both states bound to the corner of the L as well as scattering states which propagate along the arms. In Sec. VI, we summarize our main results and describe some ways of experimentally testing these results.

## II. SURFACE HAMILTONIAN

The surface states of a three-dimensional TI are governed by the massless Dirac equation. The form of the Dirac equation depends on the orientation of the surface [30,42–45]; the simplest form appears when the surface is given by the  $x$ - $y$  plane. We will also be interested in the effects of a scalar potential  $V(x,y)$  and a uniform magnetic field  $\vec{B}$  which only has a Zeeman coupling to the electrons. Including these terms, the two-component wave function  $\psi(x,y)e^{-iEt}$  of an energy eigenstate satisfies the equation

$$\left[ -iv_F(\sigma^x \partial_y - \sigma^y \partial_x) + V - \frac{g\mu}{2} \vec{\sigma} \cdot \vec{B} \right] \psi = E\psi, \quad (1)$$

where  $v_F$ ,  $\mu$ , and  $g$  denote the Fermi velocity, the Bohr magneton, and the gyromagnetic ratio, respectively. (We will set  $\hbar = 1$  in this paper.)

*Spin-momentum locking.* If both  $V$  and  $\vec{B}$  are absent, the solutions of Eq. (1) have momenta  $\vec{k} = (k_x, k_y)$  and energies  $E_{\pm} = \pm v_F \sqrt{k_x^2 + k_y^2}$ . The wave functions are given

by  $\psi e^{i(k_x x + k_y y - Et)}$ , where

$$\begin{aligned} \psi_+ &= \frac{1}{\sqrt{2}} \begin{pmatrix} 1 \\ \frac{k_y - ik_x}{E} \end{pmatrix} \text{ for } E_+, \\ \psi_- &= \frac{1}{\sqrt{2}} \begin{pmatrix} 1 \\ -\frac{k_y - ik_x}{E} \end{pmatrix} \text{ for } E_-. \end{aligned} \quad (2)$$

Upon calculating the expectation values  $\langle \sigma^x \rangle$ ,  $\langle \sigma^y \rangle$ , and  $\langle \sigma^z \rangle$ , we find that the direction of spin is perpendicular to both  $\hat{z}$  and  $\hat{k} = \vec{k}/|\vec{k}|$ , namely,  $\langle \vec{\sigma} \rangle = \hat{k} \times \hat{z}$  and  $-\hat{k} \times \hat{z}$  for  $E_+$  and  $E_-$ , respectively. This property of the surface states is called spin-momentum locking.

If we now turn on a magnetic field perpendicular to the surface,  $\vec{B} = B_z \hat{z}$ , the states with momentum  $(k_x, k_y)$  will have energies  $E_{\pm} = \pm \sqrt{v_F^2(k_x^2 + k_y^2) + (g\mu B_z/2)^2}$ ; hence there will be a gap of  $|g\mu B_z|$  at  $k = 0$ . Further, these states have a nonzero value of  $\langle \sigma^z \rangle$ .

*Effect of a potential.* Let us now turn on a potential  $V(x,y)$  but no magnetic field  $\vec{B}$ . Then Eq. (1) takes the form

$$[v_F(-i\sigma^x \partial_y + i\sigma^y \partial_x) + V(x,y)]\psi = E\psi. \quad (3)$$

Equation (3) has the following symmetries.

(i) Time-reversal symmetry  $\mathcal{T}$ : Eq. (3) remains invariant if we complex conjugate all numbers, and transform and  $\psi(x,y) \rightarrow \sigma^y \psi^*(x,y)$ . Since  $\sigma^{y*} = -\sigma^y$ , we have  $\mathcal{T}^2 = -I$ ; this implies that every energy level must have a twofold degeneracy.

(ii) Parity symmetry  $\mathcal{P}$ : if the potential is invariant under reflection in  $y$ , i.e.,  $V(x, -y) = V(x,y)$ , we have a symmetry  $\mathcal{P}$  under which  $\psi(x,y) \rightarrow \psi^*(x, -y)$ .

(iii)  $\pi$ -rotation symmetry  $\mathcal{R}$ : if the potential is invariant under a  $\pi$  rotation about the  $\hat{z}$  axis, i.e.,  $V(-x, -y) = V(x,y)$ , we have a symmetry  $\mathcal{R}$  under which  $\psi(x,y) \rightarrow \sigma^z \psi(-x, -y)$ .

If a magnetic field is applied in the  $z$  direction, time-reversal symmetry (TRS) is broken but  $\mathcal{P}$  and  $\mathcal{R}$  hold if  $V$  has both parity and rotational symmetries. There is an additional symmetry which survives if a magnetic field is applied in the  $z$  direction. Equation (1) remains invariant if we complex conjugate it, transform  $\psi \rightarrow \sigma^x \psi$ , and flip  $V \rightarrow -V$  and  $E \rightarrow -E$ . This implies that if we find a localized state with an energy  $E$  for a given potential, then if the potential is flipped, there will be a localized state with energy  $-E$  for the same value of the magnetic field. Hence both attractive and repulsive potentials can produce localized states for a Dirac electron.

In Ref. [25], the effect of a  $\delta$ -function potential barrier,  $V(y) = V_0 \delta(y)$ , was studied analytically. It was shown that this can give rise to states which propagate as plane waves in the  $x$  direction and decay exponentially as one moves away from  $y = 0$ ; these states are degenerate in energy with the surface states which exist far from the potential. The effect of a magnetic field was not studied in that work. In this paper, we want to consider the effect of more complicated and realistic potentials as well as a magnetic field applied in the  $z$  direction (which, we will show, stabilizes the localized states by gapping out the surface states). Such potentials cannot be studied analytically. We will therefore discretize the continuum Hamiltonian using a lattice, and do numerical calculations with the lattice model as discussed in the following sections.

### III. LATTICE MODEL AND FERMION DOUBLING

For a general form of the potential  $V(x, y)$ , for example in the presence of impurities, it is not possible to find the energy spectrum and wave functions analytically and one has to resort to a numerical solution. For this purpose, we assume the  $x$ - $y$  plane to be a lattice of discrete points  $\{n_x, n_y\}$  and Eq. (1) becomes

$$-\frac{1}{2}(\beta_{n_x+1, n_y} - \beta_{n_x-1, n_y}) - \frac{i}{2}(\beta_{n_x, n_y+1} - \beta_{n_x, n_y-1}) + (V_{n_x, n_y} + B)\alpha_{n_x, n_y} = E\alpha_{n_x, n_y}, \quad (4)$$

$$\frac{1}{2}(\alpha_{n_x+1, n_y} - \alpha_{n_x-1, n_y}) - \frac{i}{2}(\alpha_{n_x, n_y+1} - \alpha_{n_x, n_y-1}) + (V_{n_x, n_y} - B)\beta_{n_x, n_y} = E\beta_{n_x, n_y}, \quad (5)$$

where  $\alpha_{n_x, n_y}$  and  $\beta_{n_x, n_y}$  respectively denote the wave functions of spin- $\uparrow$  and spin- $\downarrow$  electrons at the site  $\{n_x, n_y\}$ ; we have assumed a magnetic field  $\vec{B} = B_z \hat{z}$  with  $B = -g\mu B_z/2$ . In our numerical calculations, we will work in units in which the velocity  $v_F$  and lattice spacing  $a$  are both equal to unity; at the end of Sec. V we will restore all the physical units for a topological insulator like  $\text{Bi}_2\text{Se}_3$ .

*Fermion doubling.* Equations (4) and (5) suffer from the problem of ‘‘fermion doubling.’’ To see this in the simplest possible way, consider the case when both the potential and the magnetic field are absent, i.e.,  $V = 0$  and  $B = 0$ . Translational symmetry along both  $x$  and  $y$  directions allows the solution

$$\begin{pmatrix} \alpha_{n_x, n_y} \\ \beta_{n_x, n_y} \end{pmatrix} = \begin{pmatrix} \alpha \\ \beta \end{pmatrix} e^{i(k_x n_x + k_y n_y)}. \quad (6)$$

This gives

$$\begin{aligned} [\sin(k_y) - i \sin(k_x)]\beta &= E\alpha, \\ [\sin(k_y) + i \sin(k_x)]\alpha &= E\beta, \end{aligned} \quad (7)$$

which leads to the dispersion relation

$$E = \pm \sqrt{\sin^2(k_x) + \sin^2(k_y)}. \quad (8)$$

Clearly this vanishes at four points in the Brillouin zone lying at  $(0,0)$ ,  $(0,\pi)$ ,  $(\pi,0)$ , and  $(\pi,\pi)$ , giving rise to four Dirac cones, in contrast to the continuum theory which only has one Dirac cone at  $(0,0)$ .

For the sake of completeness, we will briefly discuss one of the common ways of avoiding fermion doubling which is to add a Wilson term to the Hamiltonian. This term is proportional to  $\sigma^z$ ; it corresponds to adding  $(w/2)(\alpha_{n_x+1, n_y} + \alpha_{n_x-1, n_y} + \alpha_{n_x, n_y+1} + \alpha_{n_x, n_y-1} - 4\alpha_{n_x, n_y})$  to the left-hand side of Eq. (4) and  $-(w/2)(\beta_{n_x+1, n_y} + \beta_{n_x-1, n_y} + \beta_{n_x, n_y+1} + \beta_{n_x, n_y-1} - 4\beta_{n_x, n_y})$  to the left-hand side of Eq. (5), where  $w$  is a real parameter. The dispersion relation now becomes

$$E = \pm [\sin^2(k_x) + \sin^2(k_y) + w^2(2 - \cos(k_x) - \cos(k_y))]^{1/2}. \quad (9)$$

This reduces to Eq. (8) in the low momentum limit, but it does not vanish near the boundaries of the Brillouin zone where  $k_x$  or  $k_y$  approaches  $\pm\pi$ . We thus recover a system with only one Dirac cone lying at  $(0,0)$ .

Since the Wilson term is proportional to  $\sigma^z$ , it looks like a magnetic field in the  $z$  direction; hence it breaks some symmetries such as TRS and gives rise to various spurious effects. We will therefore *not* use such a term in our numerical calculations. Rather, we will demonstrate that we can effectively avoid the fermion doubling problem by using potentials which are sufficiently smooth so that their Fourier components rapidly approach zero as we move away from  $(0,0)$ , and they have very small components near  $(0,\pi)$ ,  $(\pi,0)$ , and  $(\pi,\pi)$ . Hence the localized states produced by such potentials receive very little contributions from the doubled fermions. Our numerical results presented below will show that choosing smooth potentials enables us to avoid the fermion doubling problem without adding a Wilson term.

*Bound states and inverse participation ratio.* In our numerical studies, we will be specially interested in states which are localized in certain regions of space. We will refer to all such states as bound states for simplicity. Bound states can be identified most easily by inverse participation ratios (IPR) of all the energy eigenstates. Let  $\psi_{i; n_x, n_y}$  be the value of the wave function at the lattice site  $(n_x, n_y)$  with the  $i$ th energy eigenvalue  $E_i$ . The normalization condition implies that

$$\sum_{n_x, n_y} |\psi_{i; n_x, n_y}|^2 = 1. \quad (10)$$

We now define

$$(\text{IPR})_i = \sum_{n_x, n_y} |\psi_{i; n_x, n_y}|^4. \quad (11)$$

The more localized the wave function of a particular state is, the higher will its IPR be. This can be understood from the following example. If a normalized wave function has the form

$$\psi_{n_x, n_y} \sim \frac{e^{-(n_x^2 + n_y^2)/\xi^2}}{\xi}, \quad (12)$$

its IPR will be proportional to  $1/\xi^2$ . Hence the state with the smallest width  $\xi$  will have the largest IPR.

### IV. NUMERICAL RESULTS IN ONE DIMENSION

We first study the energy spectrum in the presence of a potential  $V$  which is only a function of  $n_y$  on a lattice. The spectrum can be found assuming the wave function to have a momentum  $k_x$  along the  $x$  direction; this reduces it to a one-dimensional problem involving  $\psi = (\alpha_{n_y}, \beta_{n_y})^T e^{i(k_x x - Et)}$ . The eigenvalue problem is given by

$$\begin{aligned} -i \sin(k_x) \beta_{n_y} - \frac{i}{2}(\beta_{n_y+1} - \beta_{n_y-1}) + V_{n_y} \alpha_{n_y} &= E\alpha_{n_y}, \\ i \sin(k_x) \alpha_{n_y} - \frac{i}{2}(\alpha_{n_y+1} - \alpha_{n_y-1}) + V_{n_y} \beta_{n_y} &= E\beta_{n_y}. \end{aligned} \quad (13)$$

We take the potential to be a barrier which is a Gaussian with an integrated weight of

$$V_{n_y} = \frac{V_b}{\sigma \sqrt{2\pi}} e^{-(n_y - n_0)^2 / (2\sigma^2)}, \quad (14)$$

with maximum value  $V_b/(\sigma \sqrt{2\pi})$  and width  $\sigma$  (see Fig. 1). In our calculations, we will set the width  $\sigma = 2$  and vary  $V_b$ . We will take the Gaussian to be centered at  $n_y = n_0 = 151$

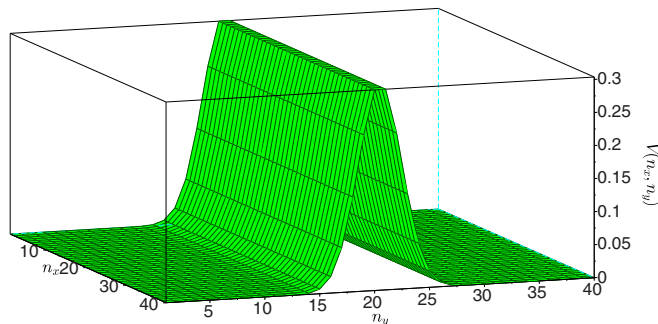


FIG. 1. (Color online) Surface plot of a potential barrier which is a Gaussian in one direction with width 2 and  $V_b = \pi/2$ , as described in Eq. (14).

for a system with 301 sites in the  $y$  direction. For  $\sigma = 2$ , the Fourier transform  $\tilde{V}_{k_y} = \sum_{n_y} e^{-ikn_y} V_{n_y}$  decreases rapidly as we go away from  $k_y = 0$  and is very small at  $k_y = \pi$ . Using the Poisson resummation formula, we obtain

$$\left| \frac{\tilde{V}_{k_y}}{\tilde{V}_{k_y=0}} \right| = \frac{\sum_{n=-\infty}^{\infty} e^{-2\pi^2\sigma^2[n-k_y/(2\pi)]^2}}{\sum_{n=-\infty}^{\infty} e^{-2\pi^2\sigma^2 n^2}}. \quad (15)$$

For  $\sigma = 2$ , we find that Eq. (15) is very well approximated by the Gaussian  $e^{-2k_y^2}$  for  $k_y$  lying in the range  $[-\pi, \pi]$ . At  $k_y = \pi$ ,  $|\tilde{V}_\pi/\tilde{V}_0| \simeq 3 \times 10^{-9}$  which is extremely small. Hence a Gaussian potential with width 2 is sufficiently smooth so that states near  $k_y = \pi$  make very little contribution to the bound states. Indeed, as mentioned below, we find numerically that the wave functions of the energy eigenstates are quite smooth, with period 2 oscillations (corresponding to components of  $k_y$  close to  $\pi$ ) being rather small.

**Bound states.** We first consider the case when no magnetic field is applied. As  $V_b$  is increased from zero, we find that a set of bound states appears which are separated from the plane wave surface states which have the gapless spectrum  $E = \pm\sqrt{k_x^2 + k_y^2}$ . The new states are plane waves along the  $x$  direction and decay exponentially as one moves away from the center of the barrier. The energy  $E$  of these states is a function of  $|k_x|$ ; this is a consequence of both the symmetries  $\mathcal{P}$  and  $\mathcal{R}$  mentioned earlier. The ratio  $dE/d|k_x|$  close to  $k_x = 0$  varies with the potential strength  $V_b$ ; it has a value of  $-v_F = -1$  close to  $V_b = 0$  and increases as  $V_b$  is increased, becoming almost zero around  $V_b = \pi/2$ . This is illustrated in the top panels of Fig. 2, with  $V_b = \pi/4$  and  $\pi/2$  in Figs. 2(a) and 2(b), respectively.  $(E/|k_x|)$  becomes positive when  $V_b$  is increased beyond  $\pi/2$ .)

We thus see that an almost flat band can be produced by tuning the barrier strength  $V_b$ . For such a band, states with different momenta can be superposed suitably to give any wave function that one chooses, and all such states will have almost the same energy. Further, such states will move only slowly in time since the group velocity  $dE/dk_x$  is close to zero.

The states bound to the potential barrier are degenerate with the surface states. In the presence of scattering (induced by, say, impurities which may be present close to the barrier), an electron occupying a bound state can scatter into a surface state. The bound states can be made immune to such scattering

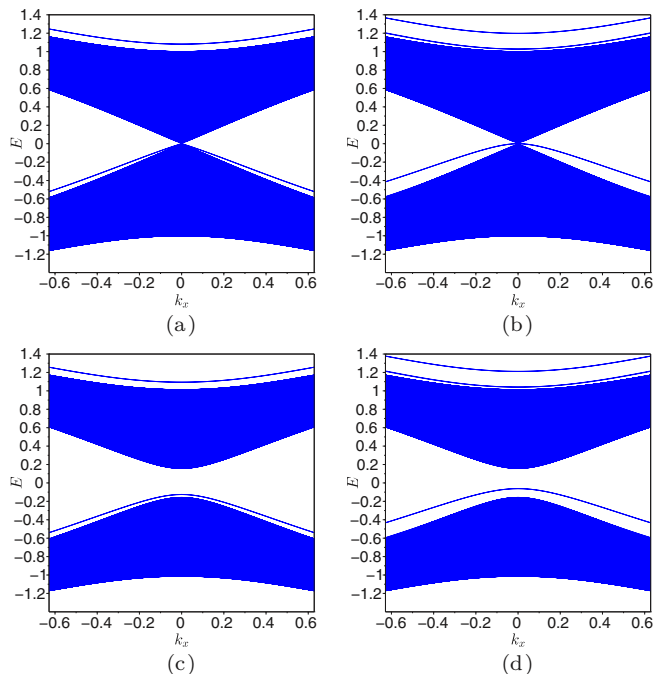


FIG. 2. (Color online) Energy dispersion of barrier states for (a)  $V_b = \pi/4$  and  $B = 0$ , (b)  $V_b = \pi/2$  and  $B = 0$ , (c)  $V_b = \pi/4$  and  $B = \pi/20$ , and (d)  $V_b = \pi/2$  and  $B = \pi/20$ , for  $k_x$  lying in the range  $[-\pi/5, \pi/5]$ .

by introducing a magnetic field. Figures 2(c) and 2(d) show the bound states when a magnetic field given by  $B = \pi/20$  is introduced. This opens a gap of  $2B$  in the spectrum of the surface states, and the bound states which lie within this gap will be robust against scattering from weak impurities by energy conservation.

We note that Figs. 2 show some additional sets of states near above the top of the band of surface states. The wave functions of these states oscillate rapidly on the scale of a lattice spacing (they have momentum components close to  $\pi$ ); hence they are lattice artifacts and have no counterparts in the continuum limit of the model.

The states produced by the potential barrier have probabilities which decay exponentially as we go away from the center of the Gaussian. The probabilities of spin- $\uparrow$  and  $\downarrow$  are given by  $|\alpha_{n_y}|^2$  and  $|\beta_{n_y}|^2$ , respectively. For  $B = 0$ , these are shown in Figs. 3(a), 3(c), and 3(e) for states with  $k_x = -\pi/10, 0$ , and  $\pi/10$ , respectively. We see that, for  $k_x = 0$ , the probability is spread over the entire range of  $n_y$ . (The probability looks like a band because it oscillates between 0 and 0.007 with period 2 in  $n_y$ .) Hence this state is not localized; this will be studied further below using the decay length.

Note that all the bound states shown in Figs. 3, namely, 3(a), 3(b), 3(d), 3(e), and 3(f), have probability profiles which are quite smooth and do not show any oscillations with period 2 in  $n_y$ . This may seem surprising since we have not added a Wilson term to gap out the low-energy fermions which exist near the momentum  $k_y = \pi$ , and we would have expected these fermions to lead to period 2 oscillations. However, since the potential is quite smooth and has only a small Fourier component near  $k_y = \pi$  as discussed after Eq. (15), the

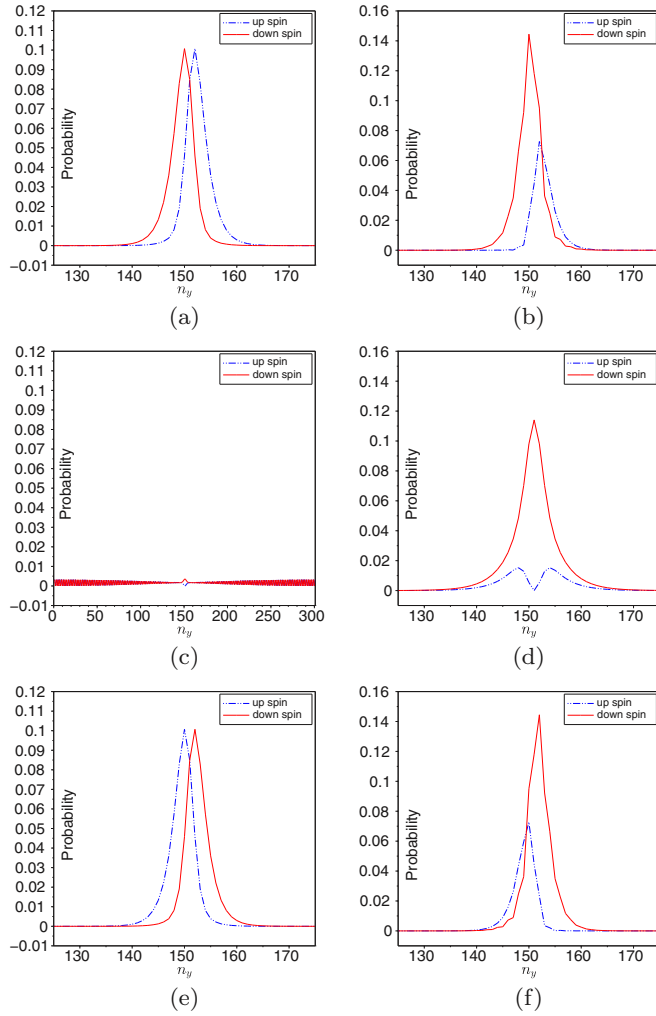


FIG. 3. (Color online) Probabilities of barrier states for  $V_b = \pi/2$  and (a)  $B = 0$ ,  $k_x = -\pi/10$ , (b)  $B = \pi/20$ ,  $k_x = -\pi/10$ , (c)  $B = 0$ ,  $k_x = 0$ , (d)  $B = \pi/20$ ,  $k_x = 0$ , (e)  $B = 0$ ,  $k_x = \pi/10$ , and (f)  $B = \pi/20$ ,  $k_x = \pi/10$ . The probabilities of spin- $\uparrow$  and  $\downarrow$  are shown in blue (dashed line) and red (solid line), respectively.

low-energy doubled fermions contribute very little to the bound states formed by the potential. This demonstrates that choosing a smooth potential profile can enable us to essentially bypass the fermion doubling problem.

For  $B = \pi/20$ , Figs. 3(b), 3(d), and 3(f) show the probabilities for  $k_x = -\pi/10$ , 0, and  $\pi/10$ , respectively. In this case, the  $k_x = 0$  state is also localized. In Figs. 3(b), 3(d), and 3(f), the spin- $\downarrow$  probabilities are larger than the spin- $\uparrow$  probabilities because of the presence of a magnetic field  $B > 0$ . In all the plots in Figs. 3 we observe that the probabilities of spin- $\uparrow$  and  $\downarrow$  get reflected about the center of the Gaussian when we change  $k_x \rightarrow -k_x$ ; this is a consequence of both the symmetries  $\mathcal{P}$  and  $\mathcal{R}$ .

**Decay length.** Since the probabilities in Figs. 3 decay rather rapidly (within a few lattice spacings), it is difficult to estimate the decay lengths accurately from these probabilities. The decay length can be estimated more easily from the IPR as follows. Since the states decay in only one direction, the probability  $|\psi^2|$  will be proportional to  $e^{-|n|/\xi}/\xi$  (where  $n$  denotes the

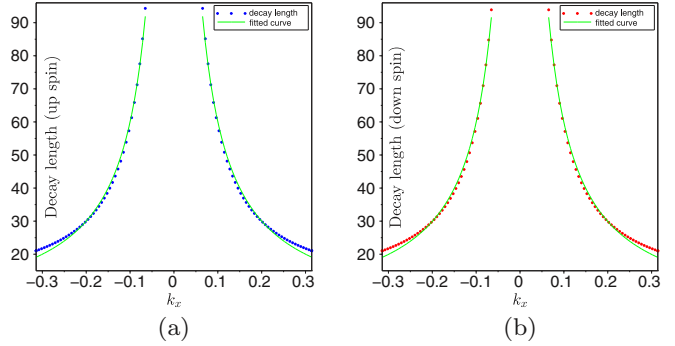


FIG. 4. (Color online) Estimates of decay length  $\xi$  (shown by asterisks) from inverse participation ratio of barrier states for  $V_b = \pi/2$  and  $B = 0$  for (a) spin- $\uparrow$  and (b) spin- $\downarrow$ . A least square fit of the form  $\xi = c/|k_x|$  (shown by green lines) gives  $c = 6.00$  for spin- $\uparrow$  and  $5.98$  for spin- $\downarrow$ .

deviation of  $n_y$  from the center of the Gaussian), and the IPR will be proportional to  $1/\xi$ . We therefore simply define the decay length  $\xi$  to be the inverse of the IPR and plot the resultant values of  $\xi$  versus the momentum  $k_x$ . We find that  $\xi$  is proportional to  $1/|k_x|$ , the constant of proportionality being almost the same for the probabilities of the spin- $\uparrow$  and  $\downarrow$  components. This is shown in Fig. 4 for  $V_b = \pi/2$  and  $B = 0$ . We observe that the decay length diverges as  $k_x \rightarrow 0$ , implying that there is no bound state at  $k_x = 0$ . Thus the spectrum of bound states does not contain the point  $k_x = 0$ . The situation is quite different when a magnetic field is present; then the decay length is finite for all values of  $k_x$  and there is a bound state even when  $k_x = 0$ .

**Local density of states.** It is useful to look at the local density of states produced by the potential barrier. For the case  $V_b = \pi/2$  and  $B = \pi/20$ , where there is an almost flat band [Fig. 2(d)], the local density of states produced by the bound states lying in the range  $-\pi/5 < k_x < \pi/5$  is defined to be

$$\rho(E, n_y) = \int_{-\pi/5}^{\pi/5} \frac{dk_x}{2\pi} \delta(E - E_{k_x}) |\psi(k_x; n_y)|^2. \quad (16)$$

This is shown in Fig. 5 where we have smoothed the  $\delta$  functions in Eq. (16) by replacing them by Gaussians with width 0.1. [We have approximated the integral in Eq. (16) by taking a large number  $N$  of equally spaced points in  $k_x$

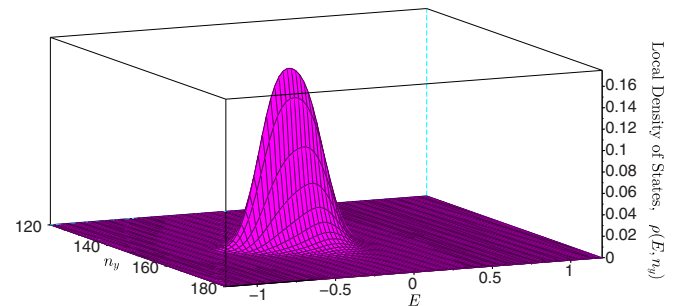


FIG. 5. (Color online) Local density of states due to bound states produced by a potential barrier with  $V_b = \pi/2$  and a magnetic field  $B = \pi/20$ . The  $\delta$  functions in energy have been replaced by Gaussians with width 0.1.

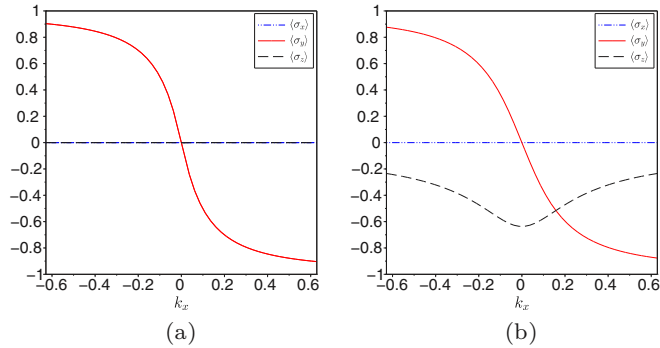


FIG. 6. (Color online) Spin expectation values of barrier states for (a)  $V_b = \pi/2$ ,  $B = 0$  and (b)  $V_b = \pi/2$ ,  $B = \pi/20$ . The  $\langle\sigma^x\rangle$ ,  $\langle\sigma^y\rangle$ , and  $\langle\sigma^z\rangle$  are shown by blue dot-dash, red solid, and black dashed lines, respectively. For  $B = 0$ ,  $\langle\sigma^x\rangle = \langle\sigma^z\rangle = 0$  coincide.

from  $-\pi/5$  to  $\pi/5$ , adding up the contributions from all those points, and dividing by  $5N$ .] As expected from Fig. 2(d), the local density of states is peaked at an energy of about  $-0.2$  and at  $n_y = 151$ , where the barrier is located.

*Spin.* It is interesting to look at the expectation values of the different components of the spin as a function of  $k_x$ . This is shown in Fig. 6 for  $V_b = \pi/2$  and (a)  $B = 0$  and (b)  $B = \pi/20$ . These figures show certain symmetries which can be understood as follows. The symmetry  $\mathcal{P}$  under which  $\psi(x, y) \rightarrow \psi^*(x, -y)$  implies that  $\langle\sigma^y\rangle$  will change sign but  $\langle\sigma^x\rangle$  and  $\langle\sigma^z\rangle$  will remain the same if we change  $k_x \rightarrow -k_x$ . The symmetry  $\mathcal{R}$  under which  $\psi(x, y) \rightarrow \sigma^z \psi(-x, -y)$  implies that  $\langle\sigma^x\rangle$  and  $\langle\sigma^y\rangle$  will change sign but  $\langle\sigma^z\rangle$  will remain the same under  $k_x \rightarrow -k_x$ . Combining these results, we see that  $\langle\sigma^x\rangle$  must be equal to zero for each value of  $k_x$  for any value of  $B$ ; this agrees with Fig. 6. Finally, if  $B = 0$ , TRS leads to all three spin expectation values changing sign under  $k_x \rightarrow -k_x$ . Combined with the symmetries  $\mathcal{P}$  or  $\mathcal{R}$ , this means that  $\langle\sigma^z\rangle$  must equal zero for each value of  $k_x$ .

To summarize this section, applying a combination of a translation invariant potential barrier and a magnetic field to Dirac electrons can produce a one-dimensional system which can be thought of as a one-band quantum wire. The dispersion of this system is unusual in that the energy is an even function of  $k_x$ , unlike chiral systems where the energy is an odd function such as  $E = vk_x$ . The dispersion can be controlled by tuning the barrier strength; in particular, the dispersion can be made almost flat. The wave functions of these states decay exponentially away from the barrier; the decay length increases as  $|k_x|$  decreases but remains finite at  $k_x = 0$  if a magnetic field is present. The expectation values of the spin components also vary with  $k_x$ . We note that all these results are in qualitative agreement with those obtained analytically in Ref. [25] for the case of a  $\delta$ -function potential barrier.

## V. NUMERICAL RESULTS IN TWO DIMENSIONS

In this section, we will present our results for three cases where the potential  $V(n_x, n_y)$  does not have translational symmetry along any direction. We will therefore use Eqs. (4) and (5) to find the spectrum for a two-dimensional system.

Apart from the symmetries  $\mathcal{T}$  (if  $B = 0$ ),  $\mathcal{P}$  [if  $V(n_x, -n_y) = V(n_x, n_y)$ ], and  $\mathcal{R}$  [if  $V(-n_x, -n_y) = V(n_x, n_y)$ ], which the continuum Hamiltonian has, Eqs. (4) and (5) have two other symmetries which are peculiar to the lattice model. Equations (4) and (5) remain invariant under a transformation  $\mathcal{A}_x$  which takes  $\psi_{n_x, n_y} \rightarrow (-1)^{n_x} \sigma^z \psi_{n_x, n_y}^*$ , and a transformation  $\mathcal{A}_y$  which takes  $\psi_{n_x, n_y} \rightarrow (-1)^{n_y} \psi_{n_x, n_y}^*$ . Combining  $\mathcal{A}_x$  and  $\mathcal{A}_y$ , we find a symmetry under the transformation  $\mathcal{A}_{xy}$  which takes  $\psi_{n_x, n_y} \rightarrow (-1)^{n_x + n_y} \sigma^z \psi_{n_x, n_y}$ . This implies that the eigenstates of the Hamiltonian can be chosen to satisfy either  $\mathcal{A}_{xy} \psi = \psi$  or  $\mathcal{A}_{xy} \psi = -\psi$ . If  $\mathcal{A}_{xy} \psi = \psi$ , the spin- $\uparrow$  (spin- $\downarrow$ ) component must be zero if  $n_x + n_y$  is odd (even), and the situation is reversed if  $\mathcal{A}_{xy} \psi = -\psi$ . Thus imposing the constraint  $\mathcal{A}_{xy} \psi = \psi$  (or  $= -\psi$ ) would eliminate half the components of  $\psi_{n_x, n_y}$ . This is equivalent to the Kogut-Susskind prescription for reducing the fermion doubling problem; the reduction is by a factor of 2 in this system [49].

However, we will *not* impose constraints of the form  $\mathcal{A}_{xy} \psi = \pm \psi$  when doing our numerical conditions since this would lead to wave functions which have large oscillations with period 2 in  $n_x$  and  $n_y$ . The various wave functions that we have found numerically and have discussed below are all quite smooth and have only small oscillations with period 2. Once again, this is because we have chosen all the potentials to have very small Fourier components near  $k_x$  or  $k_y$  equal to  $\pi$ .

*Impurity potential.* We first consider the effect of a localized potential which may arise from a nonmagnetic impurity; by localized we mean that the potential rapidly goes to zero outside some region. In particular, we will consider a Gaussian form

$$V_{\text{imp}; n_x, n_y} = \frac{V_i}{2\pi\sigma^2} e^{-[(n_x - n_0)^2 + (n_y - n_0)^2]/(2\sigma^2)}, \quad (17)$$

where  $\sigma = 2$  and  $V_i = 5\pi$ . In the absence of a magnetic field, we find numerically that this potential does not produce a bound state. However, when we turn on a magnetic field (we take  $B = \pi/20$ ), we find that a localized bound state can appear as shown in Fig. 7. (The inverse participation ratio is particularly large for states which are localized in both directions and is therefore very useful for numerically finding such states.)

We thus see that while a potential alone does not localize a Dirac electron (since an electron can Klein tunnel through a potential), a potential along with a magnetic field can localize an electron. Qualitatively, this is because a magnetic field produces a gap; if a localized potential can produce a state lying in that gap, the wave function of that state will decay exponentially as one goes far away from the potential thereby producing a localized state. This suggests that one can construct a quantum dot hosting one or more states by applying a localized potential and a magnetic field to a system of Dirac electrons. (Our results are in agreement with Ref. [50] where it is shown that a massive Dirac particle can have in-gap bound states in an isotropic Gaussian potential in two dimensions.)

*Potential barrier and impurity.* Next we consider when both a barrier and an impurity are present (both are assumed to be nonmagnetic). In the absence of a magnetic field, TRS implies that the states propagating as plane waves along the barrier will not backscatter from momentum  $+k_x$  to  $-k_x$

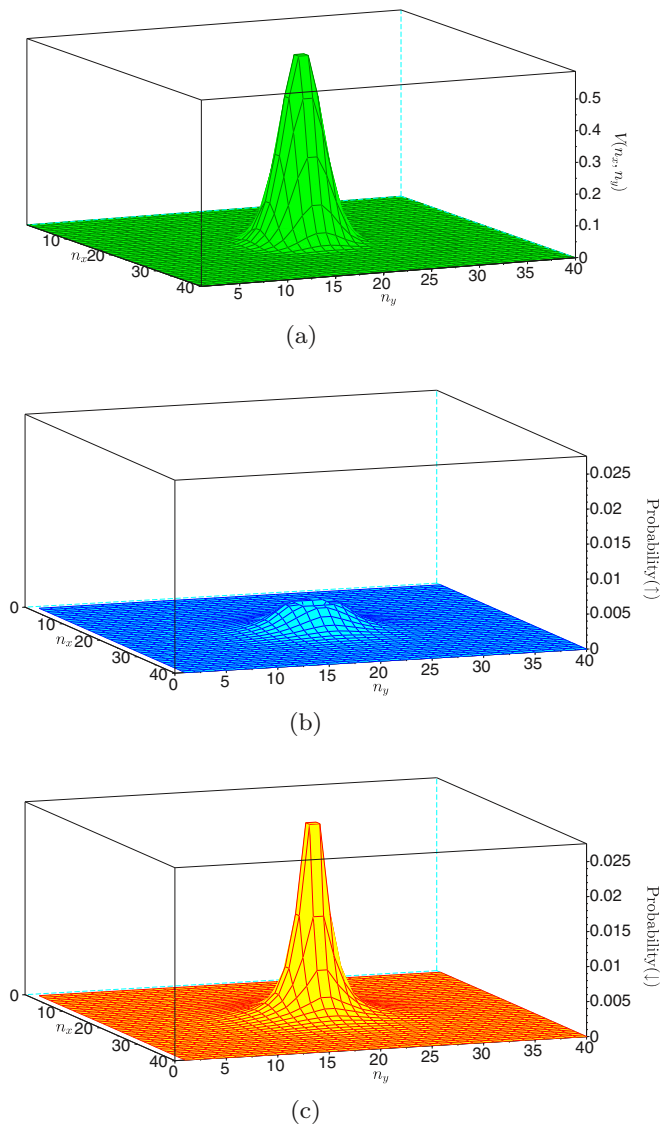


FIG. 7. (Color online) (a) Surface plot of an impurity potential which is a Gaussian with width 2 in both directions and  $V_i = 5\pi$ , as described in Eq. (17). Surface plots of probabilities of (b) spin- $\uparrow$  and (c) spin- $\downarrow$  for the bound state, for  $B = \pi/20$  and a system with  $40 \times 40$  sites. The spin- $\downarrow$  probability is much larger than the spin- $\uparrow$  probability; this is because the magnetic field points in the  $+\hat{z}$  direction.

in the presence of an impurity. Essentially this is because those two states have spins pointing in opposite directions [as shown in Fig. 6(a)], and a nonmagnetic impurity cannot flip the spin. For a weak impurity, the absence of backscattering can be shown using first order perturbation theory. For an elastic (i.e., energy conserving scattering), we only need to consider scattering between two plane wave states with equal and opposite momenta  $\pm k_x$ . Let us denote the corresponding wave functions as  $\psi_{k_x; n_x, n_y}$  and  $\psi_{-k_x; n_x, n_y}$ . Then the Born approximation in one dimension [51] shows that the reflection amplitude produced by an impurity  $V_{\text{imp}; n_x, n_y}$  is given by

$$r_{k_x} = -\frac{i}{dE/dk_x} \langle \psi_{-k_x} | V_{\text{imp}} | \psi_{k_x} \rangle. \quad (18)$$

In the absence of a magnetic field,  $\psi_{\pm}$  are related by time-reversal transformation:

$$\psi_{-k_x; n_x, n_y} = \sigma^y \psi_{k_x; n_x, n_y}^*. \quad (19)$$

Hence the matrix element in Eq. (18) is equal to

$$\langle \psi_{-k_x} | V_{\text{imp}} | \psi_{k_x} \rangle = \sum_{n_x, n_y} V_{\text{imp}; n_x, n_y} \psi_{k_x; n_x, n_y}^T \sigma^y \psi_{k_x; n_x, n_y}. \quad (20)$$

This vanishes for any form of  $V_{\text{imp}}$  because the antisymmetry of  $\sigma^y$  implies that  $\psi_{k_x; n_x, n_y}^T \sigma^y \psi_{k_x; n_x, n_y} = 0$ . Thus the barrier states are immune to scattering by weak impurities if no magnetic field is present. This also implies that an impurity cannot produce a bound state. This is because bound states in one dimension occur at the complex values of  $k_x$  where  $r_{k_x}$  has a pole (when  $r_{k_x}$  is analytically continued away from the real axis); if  $r_{k_x} = 0$  for all  $k_x$ , its analytical continuation will also be zero and it will have no pole in the complex plane.

These arguments break down when a magnetic field is present because  $\psi_{\pm k_x}$  will no longer be related to each other by Eq. (19), and  $\langle \psi_{-k_x} | V_{\text{imp}} | \psi_{k_x} \rangle$  will not be equal to zero in general; hence the reflection amplitude in Eq. (18) will no longer vanish. [To put it differently, the states at momenta  $\pm k_x$  no longer have spins pointing in opposite direction as shown in Fig. 6(b); hence a non-magnetic impurity can cause a transition between the two.] In addition, a bound state becomes possible. This is illustrated in Fig. 8 where the spin- $\uparrow$  and  $\downarrow$  probabilities are shown for a bound state which appears when there is a potential barrier and an impurity with the forms given in Eqs. (14) and (17) with  $V_b = \pi/2$  and  $V_i = \pi$ , respectively, and a magnetic field  $B = \pi/20$  is also present. The spin- $\downarrow$  probability again turns out to be much larger than the spin- $\uparrow$  probability because the magnetic field points in the  $+\hat{z}$  direction.

Assuming that a magnetic field is present and  $\langle \psi_{-k_x} | V_{\text{imp}} | \psi_{k_x} \rangle \neq 0$ , Eq. (18) implies that the reflection amplitude is larger if the group velocity  $dE/dk_x$  is smaller. This means that if the barrier strength is tuned to produce an almost flat band, even a small impurity potential will lead to a large backscattering.

We find numerically that for a given value of the magnetic field, the strength of the impurity potential which is required to produce a state bound to it is smaller when a potential barrier is present compared to the case when a potential barrier is not present. This is why we set  $V_i = \pi$  in Fig. 8 but  $V_i = 5\pi$  in Fig. 7. A qualitative reason for this is that a potential barrier already creates edge states which are localized in one direction (perpendicular to the barrier); then an impurity potential only has to localize such a state in the other direction (along the barrier). Without a potential barrier, the impurity potential by itself has to localize a bound state in two directions.

*L-shaped potential.* Finally, we give an example to show that one can create quasi-one-dimensional systems with bends which can host either localized or extended states of electrons. Figure 9 shows an L-shaped potential barrier consisting of two semi-infinite arms in perpendicular directions; each arm has the form given in Eq. (14) with  $\sigma = 2$  and  $V_b = 5\pi$ . In general, we find two kinds of states, one localized at the corner of the L and the other running along the arms. An example of a bound state localized at the corner is shown in Fig. 10.

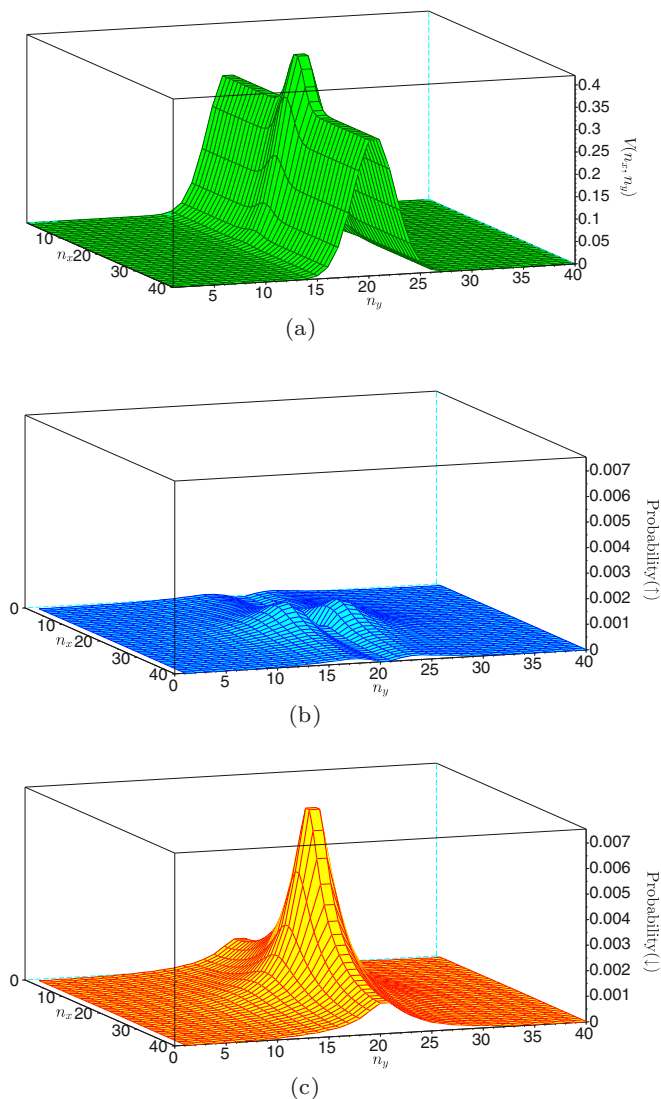


FIG. 8. (Color online) (a) Surface plot of a potential which is a combination of a barrier which is a Gaussian with width 2 and  $V_b = \pi/2$  in the transverse direction and an impurity potential which is a Gaussian with width 2 in both directions and  $V_i = \pi$ . Surface plots of probabilities of (b) spin- $\uparrow$  and (c) spin- $\downarrow$  for the bound state, for  $B = \pi/20$  and a system with  $40 \times 40$  sites.

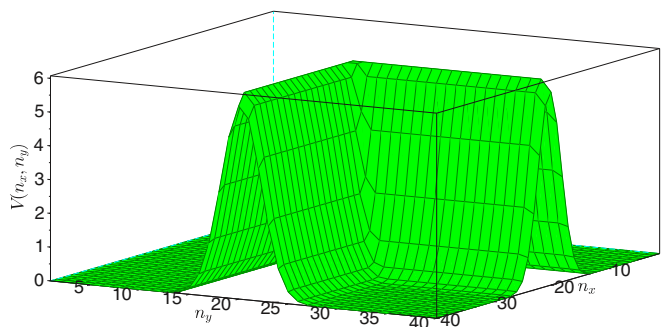


FIG. 9. (Color online) Surface plot of an L-shaped potential. The potential has a width of 2 and a maximum value of  $5\pi/(2\sqrt{2\pi})$  along the spine of the L.

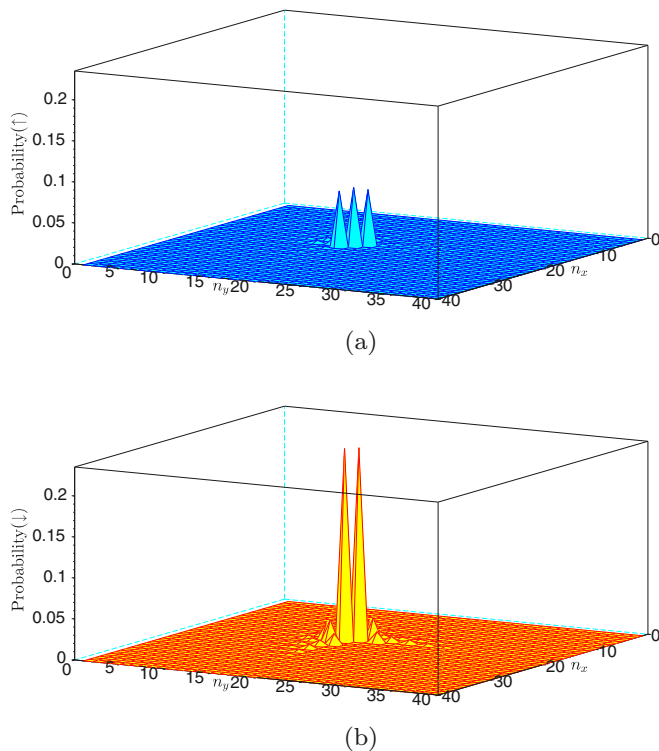


FIG. 10. (Color online) Surface plots of probabilities of (a) spin- $\uparrow$  and (b) spin- $\downarrow$  for the bound state localized at the corner of an L-shaped potential, for  $B = \pi/20$  and a system with  $40 \times 40$  sites.

Figure 11 shows an extended wave function which runs along the arms of the potential. (The spin probabilities for this state are in the form of standing waves because of reflections from the edges of the system where we have used open boundary conditions. The wave function would have been a plane wave instead of a standing wave if the system was infinitely large.) The ratio of the spin- $\downarrow$  probability to the spin- $\uparrow$  probability is much larger for the state in Fig. 10 compared to the state in Fig. 11. This is because the magnitudes of the momenta  $k_x$  and  $k_y$  (one or both of which must be complex for a state which is localized in one or both directions) turns out to be much smaller than the magnetic field  $B$  for the localized state; hence the wave function is dominated by the magnetic field and therefore has a large component in the direction opposite to it. For the extended state, however, the magnitudes of the momenta turn out to be much larger than  $B$ ; hence the wave function is much less affected by the presence of  $B$ . Indeed we find numerically that extended states are present if there is only an L-shaped potential but no magnetic field, while a bound state can appear at the corner only if a magnetic field is applied.

*Physical numbers.* We have presented all our numerical results in dimensionless units for convenience. However, we must convert these to some physical numbers in order to think of testing these results experimentally. To do this, let us fix the lattice spacing to be, say,  $a = 0.1 \mu\text{m}$ . We emphasize that we are using the lattice only as a way of discretizing the continuum Hamiltonian and studying it numerically; our lattice is *not* the lattice of the underlying material which, for  $\text{Bi}_2\text{Se}_3$ , has a spacing of about 1 nm for the quintuple

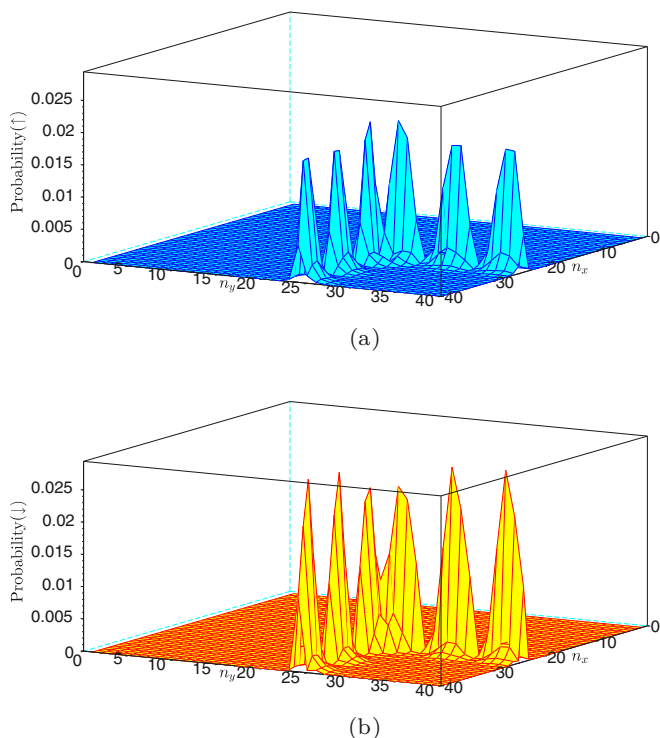


FIG. 11. (Color online) Surface plots of probabilities of (a) spin- $\uparrow$  and (b) spin- $\downarrow$  for a state which is extended along the arms of an L-shaped potential, for  $B = \pi/20$  and a system with  $40 \times 40$  sites.

layers [7]. Our lattice spacing is an arbitrary number which we choose so that the various physical parameters discussed below have experimentally realizable values. In the absence of a potential and a magnetic field, the dispersion of a massless Dirac electron with momentum  $k_x$  is given, on a lattice, by  $E = (\hbar v_F/a) \sin(k_x a)$ . For the topological insulator  $\text{Bi}_2\text{Se}_3$ , the velocity on the  $x$ - $y$  surface (perpendicular to the quintuple layers) is given by [2]  $\hbar v_F = 3.33 \text{ eV \AA}$ . This means that the values of energy on the  $y$  axis of Fig. 2 are in units of  $\hbar v_F/a = 3.33 \times 10^{-3} \text{ eV}$ , and the values of  $k_x$  on the  $x$  axis of Figs. 2, 4, and 6 are in units of  $1/a = 10 \mu\text{m}^{-1}$ . The decay length on the  $y$  axis of Fig. 4 and the  $x$  and  $y$  coordinates in various figures are all in units of  $0.1 \mu\text{m}$ . Next, a potential barrier of the form given in Eq. (14) with  $V_b = \pi/2$  and  $\sigma = 2$  corresponds to a potential whose maximum value is  $(V_b/\sigma\sqrt{2\pi})(\hbar v_F/a) = 1.04 \times 10^{-3} \text{ eV}$  and width is  $0.2 \mu\text{m}$ . Finally, the Bohr magneton  $\mu = e\hbar/(2m_e c) = 5.79 \times 10^{-5} \text{ eV/T}$ . Assuming the gyromagnetic ratio to be  $g = 2$  as for a free electron, a value of  $B = -g\mu B_z/2 = \pi/20$  corresponds to a magnetic field strength  $|B_z| = (\pi/20)(\hbar v_F/a)/(5.79 \times 10^{-5}) = 9.03 \text{ T}$ . The numbers given above should only be considered to be rough guidelines; we expect our results for the bound states and their various properties to hold for a range of parameters.

## VI. SUMMARY AND DISCUSSION

In this paper, we have used a lattice model to study how a combination of time-reversal symmetric (nonmagnetic)

potentials and a magnetic field can be used to confine Dirac electrons in different geometries. Our main results are as follows.

(i) For an infinitely long potential barrier and no magnetic field, the dispersion of the edge states propagating along the barrier is qualitatively of the form  $E = v|k_x|$ , where  $k_x$  is the momentum along the barrier, if  $|k_x|$  is much smaller than the inverse lattice spacing; note that this is quite different from a chiral dispersion which is given by  $E = vk_x$ . The expectation value of the spin,  $\langle \vec{\sigma} \rangle$ , of the edge states lies in the  $y$  direction. The velocity  $v$  of the edge states is smaller than that of the surface states and it can be varied by changing the strength of the potential barrier. The velocity  $v$  becomes very small for a particular value of the potential barrier, giving rise to an almost flat band near  $E = 0$ . The wave function of the edge states decays exponentially away from the potential barrier; the decay length is inversely proportional to  $|k_x|$ . Hence the edge states will cease to exist when the decay length becomes comparable to the size of the system.

(ii) When a Zeeman field is applied in the  $z$  direction, the surface states become gapped but the edge states do not. Further, an edge state now exists even for  $k_x = 0$ . The spin expectation value develops a component along the  $z$  direction. Since the dispersion of the edge states can be controlled by the strength of the potential barrier, the edge states define a tunable one-dimensional system which is separated from the surface states by a gap.

(iii) Next we study what happens when there is a potential localized in some region. In the absence of a Zeeman field such a potential does not produce any localized states. But when a Zeeman field is turned on, we find that exponentially localized states can appear if the potential is strong enough. This gives us a zero-dimensional system.

(iv) We then study a combination of a long potential barrier, a localized potential, and a magnetic field; we find that states can appear which are bound to the localized potential. We also study what happens if there is an L-shaped potential consisting of two semi-infinitely long arms meeting at a corner and a magnetic field. We find that there can be both states bound to the corner of the L as well as scattering states along the arms. Thus the electrons can propagate through the corner from one arm to the other.

An interesting feature of our numerical results is that the use of smooth potentials has enabled us to effectively avoid the fermion doubling problem even though we have not added a Wilson term to the Hamiltonian. The basic idea is that a smooth potential does not excite the extra fermions which therefore play no role in the formation of localized states.

Our results can be experimentally tested in a number of ways. To begin with, a potential barrier (straight or bent) can be produced by placing an appropriately shaped gate close to the surface of a TI and tuning the gate voltage. Then spin-resolved ARPES can be used to find the energy dispersion and spins of the different edge states. However, this method is not easy to use when a magnetic field is present since the field would affect the trajectories of the electrons emitted from the surface. A second method would be to measure the local density of states using the tunneling conductance from a spin-polarized STM tip which is placed very close to the barrier. If the local density of states is found to be higher when a potential barrier

is present compared to the case of no potential, this would provide evidence for the edge states. An almost flat band would give rise to a particularly large density of states at the location of the barrier. Finally, it would be interesting to measure the differential conductance of the quasi-one-dimensional system which is produced by a long potential barrier (either straight or with bends as in an L-shaped potential), and study how this varies with the potential barrier or a magnetic field; such a variation would provide indirect evidence for the edge states. Note that since the edge states carry a spin (which is different for opposite edge momenta  $+k_x$  and  $-k_x$ ), a nonzero charge conductance along the barrier would also imply a nonzero spin conductance.

We end by pointing out some directions for future work. We have only considered the effects of a Zeeman coupling to a magnetic field in this work. A magnetic field that has only a Zeeman coupling and no orbital coupling can be realized in a TI by doping with magnetic impurities [52] or by depositing a ferromagnetic layer on the surface [53]. However, one should, in general, study the effects of the orbital coupling of electrons to a magnetic field. In a lattice model, such a coupling can be introduced through the phase in the couplings between nearest neighbor sites following the Peierls prescription.

Our work has shown that in the presence of a magnetic field, one can use potentials of various shapes to form wave guides along which Dirac electrons can propagate. An important issue that we have explored is whether the various kinks in the potential (such as a localized potential on a barrier, or the corner of an L-shaped potential) allow electrons to travel along the entire length of the barrier, or whether they backscatter the electrons so strongly that states can only exist on a part of the barrier. For the L-shaped potential, for instance, Fig. 11 shows

a state which exists on both arms of the L; this shows that the corner of the L does not reflect an electron completely.

If we can fully understand the effects of each of the potentials considered in this paper, we may try to construct a network of wave guides by laying down a number of appropriately shaped gates on the surface of a topological insulator and then applying the required potentials to the gates. For this purpose it would be useful to study the scattering matrix and conductance of quasi-one-dimensional systems with L-shaped bends and “T” junctions. We would like to mention here that L-shaped geometries have been theoretically proposed for probing the edge states of a two-dimensional TI [54], and gates of different shapes have been experimentally fabricated in a two-dimensional TI [9]. Thus gates of various shapes are both experimentally realizable and theoretically interesting in TI systems.

Finally, it would be interesting to study the effect of electron-electron interactions. The almost flat band of states that can be produced by tuning the barrier potential can be a platform for hosting a variety of strongly correlated electron states. In this connection we would like to mention some recent papers where it has been shown that magnetic impurities or barriers and interactions between electrons can lead to oscillations in the spin density and can have measurable effects on transport at the edge of a two-dimensional topological insulator [55].

#### ACKNOWLEDGMENTS

We thank Sourin Das, Oindrila Deb, and Abhiram Soori for discussions. D.S. thanks DST, India for support under Grant No. SR/S2/JCB-44/2010.

- 
- [1] M. Z. Hasan and C. L. Kane, *Rev. Mod. Phys.* **82**, 3045 (2010).  
 [2] X.-L. Qi and S.-C. Zhang, *Rev. Mod. Phys.* **83**, 1057 (2011).  
 [3] B. A. Bernevig, T. L. Hughes, and S.-C. Zhang, *Science* **314**, 1757 (2006); B. A. Bernevig and S.-C. Zhang, *Phys. Rev. Lett.* **96**, 106802 (2006).  
 [4] L. Fu, C. L. Kane, and E. J. Mele, *Phys. Rev. Lett.* **98**, 106803 (2007); R. Roy, *Phys. Rev. B* **79**, 195322 (2009); J. E. Moore and L. Balents, *ibid.* **75**, 121306 (2007).  
 [5] C. L. Kane and E. J. Mele, *Phys. Rev. Lett.* **95**, 226801 (2005); **95**, 146802 (2006).  
 [6] J. C. Y. Teo, L. Fu, and C. L. Kane, *Phys. Rev. B* **78**, 045426 (2008).  
 [7] X. L. Qi, T. L. Hughes, and S. C. Zhang, *Phys. Rev. B* **78**, 195424 (2008); H. Zhang, C.-X. Liu, X.-L. Qi, X. Dai, Z. Fang, and S.-C. Zhang, *Nat. Phys.* **5**, 438 (2009); C.-X. Liu, X.-L. Qi, H. J. Zhang, X. Dai, Z. Fang, and S.-C. Zhang, *Phys. Rev. B* **82**, 045122 (2010).  
 [8] Y. L. Chen, J. G. Analytis, J.-H. Chu, Z. K. Liu, S.-K. Mo, X. L. Qi, H. J. Zhang, D. H. Lu, X. Dai, Z. Fang, S. C. Zhang, I. R. Fisher, Z. Hussain, and Z.-X. Shen, *Science* **325**, 178 (2009); T. Zhang, P. Cheng, X. Chen, J.-F. Jia, X. Ma, K. He, L. Wang, H. Zhang, X. Dai, Z. Fang, X. Xie, and Q.-K. Xue, *Phys. Rev. Lett.* **103**, 266803 (2009).  
 [9] M. König, S. Wiedmann, C. Brüne, A. Roth, H. Buhmann, L. W. Molenkamp, X.-L. Qi, and S.-C. Zhang, *Science* **318**, 766 (2007); M. König, H. Buhmann, L. W. Molenkamp, T. L. Hughes, C.-X. Liu, X.-L. Qi, and S.-C. Zhang, *J. Phys. Soc. Jpn.* **77**, 031007 (2008).  
 [10] D. Hsieh, D. Qian, L. Wray, Y. Xia, Y. S. Hor, R. J. Cava, and M. Z. Hasan, *Nature (London)* **452**, 970 (2008); Y. Xia, D. Qian, D. Hsieh, L. Wray, A. Pal, H. Lin, A. Bansil, D. Grauer, Y. S. Hor, R. J. Cava, and M. Z. Hasan, *Nat. Phys.* **5**, 398 (2009); Y. Xia, D. Qian, D. Hsieh, R. Shankar, H. Lin, A. Bansil, A. V. Fedorov, D. Grauer, Y. S. Hor, R. J. Cava, and M. Z. Hasan *arXiv:0907.3089*.  
 [11] D. Hsieh, Y. Xia, D. Qian, L. Wray, J. H. Dil, F. Meier, L. Patthey, J. Osterwalder, A. V. Fedorov, H. Lin, A. Bansil, D. Grauer, Y. S. Hor, R. J. Cava, and M. Z. Hasan, *Nature (London)* **460**, 1101 (2009); P. Roushan, J. Seo, C. V. Parker, Y. S. Hor, D. Hsieh, D. Qian, A. Richardella, M. Z. Hasan, R. J. Cava, and A. Yazdani, *ibid.* **460**, 1106 (2009); D. Hsieh, Y. Xia, L. Wray, D. Qian, A. Pal, J. H. Dil, J. Osterwalder, F. Meier, G. Bihlmayer, C. L. Kane, Y. S. Hor, R. J. Cava, and M. Z. Hasan, *Science* **323**, 919 (2009).  
 [12] S. Mondal, D. Sen, K. Sengupta, and R. Shankar, *Phys. Rev. Lett.* **104**, 046403 (2010); *Phys. Rev. B* **82**, 045120 (2010).

- [13] A. A. Zyuzin, M. D. Hook, and A. A. Burkov, *Phys. Rev. B* **83**, 245428 (2011).
- [14] L. Fu, *Phys. Rev. Lett.* **103**, 266801 (2009).
- [15] L. Fu and C. L. Kane, *Phys. Rev. Lett.* **100**, 096407 (2008).
- [16] A. R. Akhmerov, J. Nilsson, and C. W. J. Beenakker, *Phys. Rev. Lett.* **102**, 216404 (2009).
- [17] Y. Tanaka, T. Yokoyama, and N. Nagaosa, *Phys. Rev. Lett.* **103**, 107002 (2009); J. Linder, Y. Tanaka, T. Yokoyama, A. Sudbo, and N. Nagaosa, *ibid.* **104**, 067001 (2010).
- [18] T. Yokoyama, Y. Tanaka, and N. Nagaosa, *Phys. Rev. Lett.* **102**, 166801 (2009).
- [19] A. A. Burkov and D. G. Hawthorn, *Phys. Rev. Lett.* **105**, 066802 (2010); O. V. Yazyev, J. E. Moore, and S. G. Louie, *ibid.* **105**, 266806 (2010); K. Nomura and N. Nagaosa, *Phys. Rev. B* **82**, 161401 (2010); T. Yokoyama, J. Zang, and N. Nagaosa, *ibid.* **81**, 241410(R) (2010).
- [20] I. Garate and M. Franz, *Phys. Rev. Lett.* **104**, 146802 (2010); *Phys. Rev. B* **81**, 172408 (2010).
- [21] K. Saha, S. Das, K. Sengupta, and D. Sen, *Phys. Rev. B* **84**, 165439 (2011).
- [22] M. Guigou and J. Cayssol, *Phys. Rev. B* **82**, 115312 (2010).
- [23] R. W. Reinthaler, P. Recher, and E. M. Hankiewicz, *Phys. Rev. Lett.* **110**, 226802 (2013).
- [24] R. Takahashi and S. Murakami, *Phys. Rev. Lett.* **107**, 166805 (2011).
- [25] D. Sen and O. Deb, *Phys. Rev. B* **85**, 245402 (2012); **86**, 039902(E) (2012).
- [26] C. Wickles and W. Belzig, *Phys. Rev. B* **86**, 035151 (2012).
- [27] R. R. Biswas and A. V. Balatsky, *Phys. Rev. B* **83**, 075439 (2011).
- [28] M. Alos-Palop, R. P. Tiwari, and M. Blaauboer, *Phys. Rev. B* **87**, 035432 (2013).
- [29] M. Sitte, A. Rosch, E. Altman, and L. Fritz, *Phys. Rev. Lett.* **108**, 126807 (2012).
- [30] F. Zhang, C. L. Kane, and E. J. Mele, *Phys. Rev. B* **86**, 081303(R) (2012); *Phys. Rev. Lett.* **110**, 046404 (2013).
- [31] V. M. Apalkov and T. Chakraborty, *Europhys. Lett.* **100**, 17002 (2012); **100**, 67008 (2012).
- [32] T. Habe and Y. Asano, *Phys. Rev. B* **88**, 155442 (2013).
- [33] S. Modak, K. Sengupta, and D. Sen, *Phys. Rev. B* **86**, 205114 (2012).
- [34] A. Soori, O. Deb, K. Sengupta, and D. Sen, *Phys. Rev. B* **87**, 245435 (2013).
- [35] A. Rüegg, S. Coh, and J. E. Moore, *Phys. Rev. B* **88**, 155127 (2013).
- [36] B. Zhou, H.-Z. Lu, R.-L. Chu, S.-Q. Shen, and Q. Niu, *Phys. Rev. Lett.* **101**, 246807 (2008); H.-Z. Lu, W.-Y. Shan, W. Yao, Q. Niu, and S.-Q. Shen, *Phys. Rev. B* **81**, 115407 (2010).
- [37] J. Linder, T. Yokoyama, and A. Sudbo, *Phys. Rev. B* **80**, 205401 (2009).
- [38] R. Egger, A. Zazunov, and A. L. Yeyati, *Phys. Rev. Lett.* **105**, 136403 (2010).
- [39] A. Medhi and V. B. Shenoy, *J. Phys.: Condens. Matter* **24**, 355001 (2012).
- [40] A. Pertsova and C. M. Canali, [arXiv:1311.0691](https://arxiv.org/abs/1311.0691).
- [41] M. Neupane, A. Richardella, J. Sanchez-Barriga, S.-Y. Xu, N. Alidoust, I. Belopolski, C. Liu, G. Bian, D. M. Zhang, D. Marchenko, A. Varykhalov, O. Rader, M. Leandersson, T. Balasubramanian, T.-R. Chang, H.-T. Jeng, S. Basak, H. Lin, A. Bansil, N. Samarth, and M. Z. Hasan, [arXiv:1307.5485](https://arxiv.org/abs/1307.5485).
- [42] P. G. Silvestrov, P. W. Brouwer, and E. G. Mishchenko, *Phys. Rev. B* **86**, 075302 (2012).
- [43] L. Barreto, W. Simoes e Silva, M. Stensgaard, S. Ulstrup, X.-G. Zhu, M. Bianchi, M. Dendzik, and P. Hofmann, [arXiv:1302.0396](https://arxiv.org/abs/1302.0396).
- [44] U. Khanna, S. Pradhan, and S. Rao, *Phys. Rev. B* **87**, 245411 (2013).
- [45] O. Deb, A. Soori, and D. Sen, [arXiv:1401.1027](https://arxiv.org/abs/1401.1027) [*J. Phys.: Condens. Matter*. (to be published)].
- [46] H. Peng, K. Lai, D. Kong, S. Meister, Y. Chen, X.-L. Qi, S.-C. Zhang, Z.-X. Shen, and Y. Cui, *Nat. Mater.* **9**, 225 (2010).
- [47] Y. Okada, W. Zhou, C. Dhital, D. Walkup, Y. Ran, Z. Wang, S. D. Wilson, and V. Madhavan, *Phys. Rev. Lett.* **109**, 166407 (2012).
- [48] Y. Ran, Y. Zhang, and A. Vishwanath, *Nat. Phys.* **5**, 298 (2009).
- [49] J. Kogut and L. Susskind, *Phys. Rev. D* **11**, 395 (1975).
- [50] J. Lu, W.-Y. Shan, H.-Z. Lu, and S.-Q. Shen, *New J. Phys.* **13**, 103016 (2011).
- [51] A. Agarwal and D. Sen, *Phys. Rev. B* **73**, 045332 (2006).
- [52] K. Nomura and N. Nagaosa, *Phys. Rev. Lett.* **106**, 166802 (2011); C. Niu, Y. Dai, M. Guo, W. Wei, Y. Ma, and B. Huang, *Appl. Phys. Lett.* **98**, 252502 (2011); Y. H. Choi, N. H. Jo, K. J. Lee, J. B. Yoon, C. Y. You, and M. H. Jung, *J. Appl. Phys.* **109**, 07E312 (2011); P. Haazen, J. Laloë, T. Nummy, H. Swagten, P. Jarillo-Herrero, D. Heiman, and J. Moodera, *Appl. Phys. Lett.* **100**, 082404 (2012).
- [53] T. Yokoyama, Y. Tanaka, and N. Nagaosa, *Phys. Rev. B* **81**, 121401(R) (2010); H. Ji, J. M. Allred, N. Ni, J. Tao, M. Neupane, A. Wray, S. Xu, M. Z. Hasan, and R. J. Cava, *ibid.* **85**, 165313 (2012); Q. Meng, S. Vishveshwara, and T. L. Hughes, *Phys. Rev. Lett.* **109**, 176803 (2012).
- [54] C.-Y. Hou, E.-A. Kim, and C. Chamon, *Phys. Rev. Lett.* **102**, 076602 (2009).
- [55] Q. Meng, T. L. Hughes, M. J. Gilbert, and S. Vishveshwara, *Phys. Rev. B* **86**, 155110 (2012); R. Ilan, J. Cayssol, J. H. Bardarson, and J. E. Moore, *Phys. Rev. Lett.* **109**, 216602 (2012); C. Timm, *Phys. Rev. B* **86**, 155456 (2012); G. Dolcetto, N. Traverso Ziani, M. Biggio, F. Cavaliere, and M. Sasseti, *ibid.* **87**, 235423 (2013); *Phys. Status Solidi RRL* **7**, 1059 (2013).